Characteristics of a low repetition rate passively mode-locked Yb-doped fiber laser in an all-normal dispersion cavity

2013 Laser Phys. 23 025103

(http://iopscience.iop.org/1555-6611/23/2/025103)

Laser Phys. **23** (2013) 025103 (5pp) doi:10.1088/1054-660X/23/2/025103

Characteristics of a low repetition rate passively mode-locked Yb-doped fiber laser in an all-normal dispersion cavity

Ja-Hon Lin[1], Jia-Liang Jhu[1], Siao-Shan Jyu[2], Ting-Chun Lin[1] and Yinchieh Lai[2]

[1] Department of Electro-Optical Engineering and Institute of Electro-Optical Engineering, National Taipei University of Technology, Taipei 10608, Taiwan
[2] Department of Photonics and Institute of Electro-Optical Engineering, National Chiao-Tung University, Hsinchu 30000, Taiwan

E-mail: jhlin@ntut.edu.tw (Ja-Hon Lin)

Received 5 September 2012, in final form 12 October 2012
Published 19 December 2012
Online at stacks.iop.org/LP/23/025103

Abstract
The lasing characteristics of a 365 kHz low repetition rate Yb-doped fiber laser operated in an all-normal dispersion cavity and mode-locked by the nonlinear polarization rotation mechanism are investigated in detail. As the pump power increases, the laser exhibits two transition routes when evolved from the continuous-wave (CW) state to the mode-locked (ML) state. In one evolution route the *Q*-switched mode-locked (QML) state is sandwiched between the CW and ML states, whereas in the other more interesting evolution route the hysteresis transition between the CW and ML states is found for the first time. Under the mode-locking operation, the laser generates sub-nanosecond pulses with linear dependence of pulsewidth on bandwidth under different pump powers, indicating the presence of giant linear chirps on the laser output pulses.

(Some figures may appear in colour only in the online journal)

1. Introduction

Because of the various advantages including high power conversion efficiency, great stability, compact cavity design and easier alignment, the applications of mode-locked fiber lasers have become more popular and important. Due to its broad gain bandwidth and relatively high slope efficiency, ytterbium-doped fiber (YDF) has attracted much attention as a gain medium to be a new candidate for novel wavelength tunable lasers or delivering high energy short pulses around 1 μm. An ultrabroadband fiber reflector based on commercially available circulators has been proposed to produce a wide wavelength tuning band greater than 90 nm in a Yb-doped fiber laser (YDFL) [1]. Besides, there have been a lot of research efforts in the development of mode-locked fiber laser technologies to increase the pulse energy directly from the laser as much as possible so that the subsequent external optical amplification can be reduced or even avoided. In contrast to the stretched pulse scheme commonly employed in the laser cavity with an anomalous dispersion region [2], the self-similar pulse scheme has been demonstrated in a YDFL with a net normal dispersion cavity to achieve pulse energy above 10 nJ [3]. Moreover, many investigations have been focused to utilize fiber laser cavities with all-normal dispersion for producing dissipative solitons (DSs) through the use of numerous mode-locking techniques including the semiconductor saturable absorber mirror (SESAM) [4], carbon nanotube [5], graphene [6], nonlinear amplifying loop mirror [7], and nonlinear polarization rotation (NPR) mechanism [8–10]. With some free space optical elements inside a fiber laser cavity of all-normal dispersion, Chong *et al* have demonstrated a mode-locked YDFL with pulse energy higher than 20 nJ [9]. However, there are still inherent benefits to operating the mode-locked laser in an all-fiber

configuration. Along this development route, a number of reported works have shown that sub-mega hertz low repetition rate pulses with higher pulse energies can be generated by simply fusing long-length fibers inside the cavity to increase the cavity length [11–15]. For Yb-doped fiber lasers, 191 kHz and 187 kHz low repetition pulses were produced with the SESAM scheme, where the mode-locked optical spectrum has sub-nanometer bandwidth [11, 12]. By the NPR scheme, Kong *et al* generated 217.4 kHz low repetition pulses with bandwidth and pulsewidth of 1.7 nm and 2.8 ns respectively [13]. Broadened spectral bandwidth over 50 nm has also been experimentally demonstrated in a 690 kHz low repetition rate Yb-doped fiber laser by the NPR scheme with the measured pulsewidth over 10 ns [14]. The recorded low repetition of a mode-locked fiber laser of about 37 kHz was experimentally demonstrated by Kobtsev *et al* with an 8 km long cavity length to produce 4 μJ output pulse energy [15].

In contrast to conventional solitons operated in the anomalous dispersion region, dissipative solitons (DSs) exist in non-conservative or dissipative systems with a variety of interesting dynamics. Due to the dissipation of energy for DSs in the laser system, a continuous energy supply from an external source is needed. The interplay of all the gain and loss mechanisms is thus important to stabilize the pulses in the laser cavity. Therefore, the characteristics of the DSs including the pulse shape and width will obviously depend on the system parameters and may exhibit unique properties. As reported, square profile DSs [16] and multiple DSs [4, 17] have both been demonstrated in Er-doped and Yb-doped fiber lasers operated in the all-normal dispersion region. A numerical simulation has been used by Kobtsev *et al* to find the golden mean of cavity length to produce a high energy single pulse in ML YDFL by NPR [18]. However, the behavior of DSs produced in mode-locked Yb-doped fiber lasers with relatively low repetition rates is still very interesting and needed to be further investigated. In the present work, the characteristics of an all-normal dispersion low repetition rate YDFL mode-locked by the NPR mechanism are studied in detail. As the pump power increases, two different evolution routes from the CW to the ML state are observed and an interesting intermediate QML state as well as a hysteretic CW-to-ML transition are found. The relation between the mode-locked spectral bandwidth and the measured pulsewidth also reveals the giant chirp pulse characteristics in such a long-length all-normal dispersion cavity.

2. Experimental setup

The schematic setup of our all-normal dispersion Yb-doped fiber ring oscillator is similar to the previous report in [14]. The passive mode-locked Yb-doped oscillator is based on the NPE mechanism that relies on an in-line polarizer (ILP) and two polarization controllers (PCs). A 2.2 m long Yb-doped fiber (core diameter = 5 m) is used as the gain medium. The 976 nm LD is used as the pumping source, which is coupled into the laser cavity by a wavelength-division multiplexing (WDM) fiber coupler. A polarization-independent isolator is used to ensure uni-directional operation of the laser cavity. Besides, an isolator is connected externally to prevent the feedback of output lights into the oscillator. A section of 520 m long Hi-1060 SMF is used inside the laser cavity to increase the total cavity length for lowering the pulse repetition rate. A 90/10 fiber coupler is used as the output coupler and a 95/5 coupler is connected after the isolator as a beam splitter, from which 5% of the output light is measured by the OSA (Agilent 86146B) or the oscilloscope (Wave Surfer 62 Xs, bandwidth 650 MHz, LeCroy) to monitor the lasing dynamics.

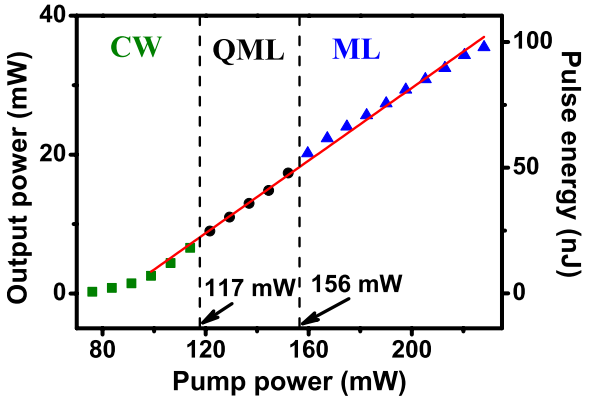

Figure 1. Laser output power and pulse energy versus pump power (route 1).

3. Results and discussion

In order to produce high energy pulses, we choose the output coupler ratio to be 90/10. Figure 1 shows the measured output powers and the estimated pulse energies versus the pump powers. The operation state of the laser will transfer from the CW state (green squares) to the intermediate QML state (black circles) and finally to the ML state (blue triangles) as the pump power increases. At the 228 mW pump power, the highest output power is about 35.5 mW and the corresponding 97.3 nJ highest pulse energy is obtained. By linear fitting (red curve), the slope efficiency is 25.3%.

The QML operation state has been observed in diode-pumped solid-state lasers (DPSSLs) and Yb-doped fiber lasers by means of a passive modulator such as the semiconductor saturable absorber mirror [4, 19] or an active modulator such as the acousto-optic modulator [20, 21]. As from the experimental reports [4, 19] and theoretical prediction [22], by means of a saturable absorber, the QML state can be observed before the complete ML pulse generation in DPSSL with SESAM. Figures 2(a)–(d) show the optical spectra and time traces of the QML pulses at 129 mW and 152 mW pump powers respectively. As the pump power increases, the 3 dB bandwidth $\Delta\lambda$ will increase from 2.9 to 5.8 nm but the central wavelength λ_0 is still around 1028 nm, as shown in figures 2(a) and (c). Besides, the interval between Q-switched envelopes will reduce from 197.1 to 153.6 μs and the repetition rate (R_{ep}) will increase from 5.1 to 6.5 kHz.

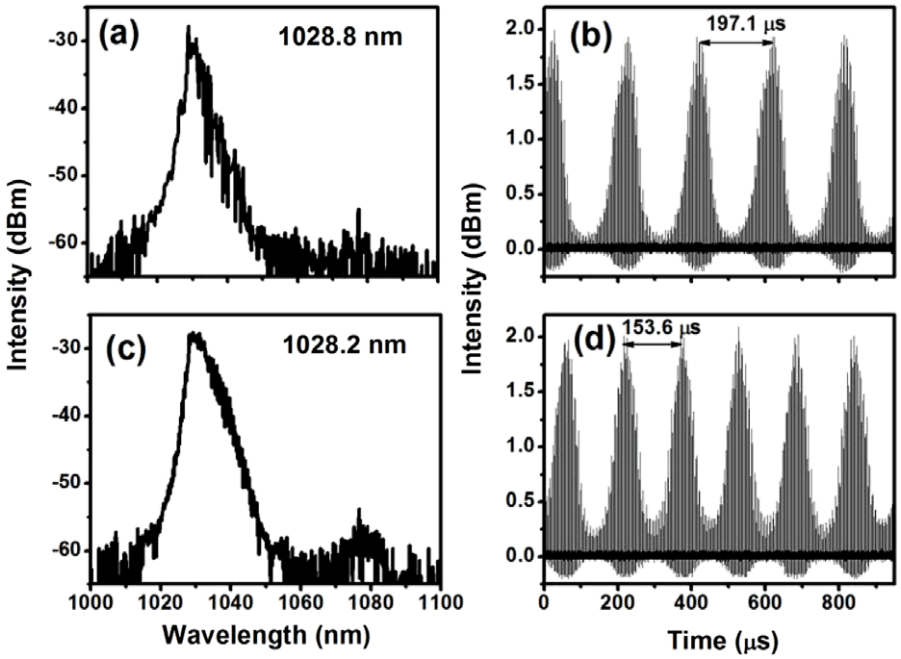

Figure 2. (a) Optical spectrum and (b) time trace of QML pulses at pump power 129 mW and (c) optical spectrum and (d) time trace of QML pulses at pump power 152 mW.

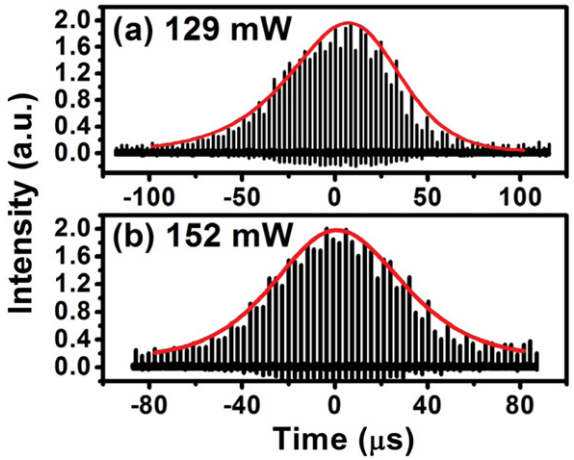

Figure 3. Expanded single QML envelope at (a) 129 mW and (b) 152 mW (red curve: fitting curve).

Figures 3(a) and (b) show the expanded time traces of a single QML envelope under which the mode-locked pulses can be obviously seen. By fitting with the formula [21]

$$I = \frac{I_0}{[e^{\frac{1.76t}{t_1}} + e^{-\frac{1.76t}{t_2}}]^2}, \quad (1)$$

where I_0 is a scaling factor and t_1 and t_2 are the rising time and falling time respectively, the temporal width of the QML envelope can be defined as $\tau = (t_1 + t_2)/2$. From the fitting, t_1 and t_1 are about 92 and 52 μs at 129 mW pump power and become 69 and 60 μs at 152 mW. Therefore, the measured QML pulsewidths are about 72 μs and 65 μs respectively. All the parameters obtained from the QML state are listed in table 1.

Table 1. Obtained parameters for the QML pulses.

P_p (mW)	λ_0 (nm)	$\Delta\lambda$ (nm)	R_{ep} (kHz)	t_1 (μs)	t_2 (μs)	τ (μs)
129	1028.8	2.9	5.1	92	52	72
152	1028.2	5.8	6.5	69	60	65

After adjusting the polarization controllers, a different evolution route from the CW to the ML state can be found. For the new transition route, the output power (left column) and the estimated pulse energy (right column) of mode-locked pulses as the pumping power P_p increases are plotted in figure 4. Here, most interestingly, the transition from the CW to the ML state as the pump power increases or decrease exhibits the hysteresis characteristics. As the pump power increases, the laser output power at the CW state (green triangles) will increase almost linearly and transfer to the ML state (blue squares) suddenly at $P_p = 205$ mW with a sudden power jump. The highest laser output power of 34.5 mW can be obtained, corresponding to the 94.3 nJ pulse energy, when the pumping power increases to 258 mW. As the pump power descends from the highest pump power, the laser output power will also decrease almost linearly and return to the CW state at the lower pump power $P_p = 183$ mW with a sudden power drop. By linear fitting (red curve), the slope efficiency of the CW state is 14.7%, and the slope efficiency of the ML state is 16.3%. It is noteworthy that, in addition to the higher output powers as the YDFL transits from CW to ML state, the slope efficiency at the ML state is also higher than that at the CW state. We believe this is because the nonlinear polarization rotation mechanism is equivalent to a fast saturable absorber, which makes the ML operation state suffer smaller loss than the CW operation state.

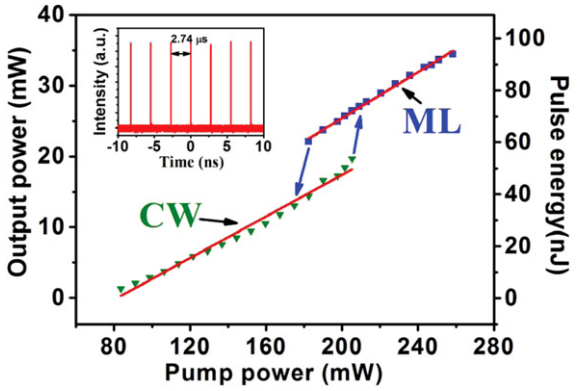

Figure 4. Laser output power and pulse energy versus pump power (route 2). Red curve: fitting curve. Slope efficiency: 14.7% (CW), 16.3% (ML). The inset shows the ML time trace.

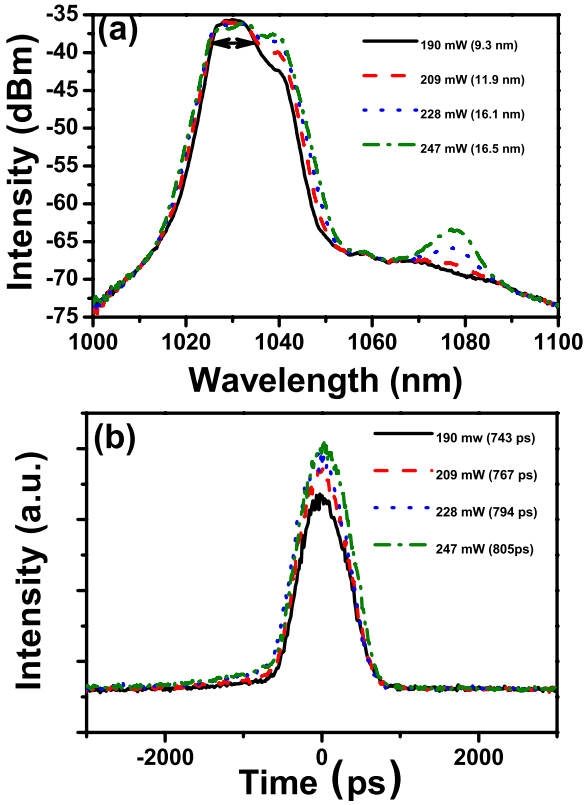

Figure 5. (a) Optical spectra and (b) time shapes of mode-locked pulses at different pump powers.

The optical spectra and time shapes of the mode-locked pulses measured by the OSA and 20 GHz high resolution oscilloscope (Agilent DCA-J 86100C) under different pump powers are shown in figures 5(a) and (b). Unlike the previous mode-locked laser, which used a 50/50 coupler and had two obvious spectral humps occurring around 1030 and 1080 nm [14], the central wavelength of the present mode-locked laser is only at 1030 nm and one of the optical spectral humps on the longer wavelength side disappears at lower pump powers. Because the YDFL has a larger stimulated emission cross section around 1030 nm, which decays quickly

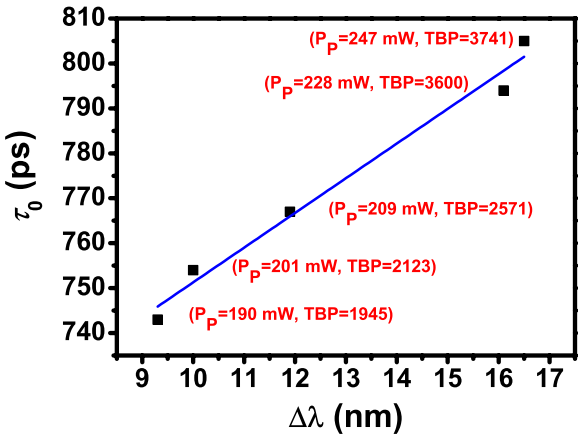

Figure 6. Pulsewidth versus bandwidth at different pump powers (blue line: linear fitting curve).

at longer exciting wavelengths, the gain of the laser at longer wavelengths does not exceed the loss to produce net stimulated emission radiation with the use of the 90% higher output coupler in the present work. As the pump power increases from 190 to 247 mW, the 3 dB bandwidth increases from 9.3 to 16.5 nm. In addition, emission around 1080 nm will be gradually generated at higher pump powers due to the four-level transition of Yb-doped fibers. Figure 5(b) shows that the pulsewidth will increase from 743 to 805 ps when the pump power rises from 190 to 247 mW. The time trace of the ML pulse train is shown in the inset of figure 4. It reveals that the time interval of sequential pulses is about 2.74 μs, which corresponds to the 365 kHz pulse repetition rate.

The relation between the measured pulsewidth τ_0 and spectral bandwidth $\Delta\lambda$ of mode-locked pulses as illustrated in figure 5 can be plotted in figure 6. The corresponding pump power and the time–bandwidth product (TBP) are also labeled on the plot. It is clear that the pulsewidth increases almost linearly, following the rise of the spectral bandwidth as the pumping power increases, and can be fitted with the straight blue line. Without any anomalous dispersion element inside this fiber laser cavity for dispersion compensation, the pulses exhibit giant chirps due to the accumulated effects of normal dispersion when propagating inside the relatively long cavity. This is why the estimated TBP is relatively large. The estimated time–bandwidth product increases from 1945 to 3741 as the pump power increases from 190 to 247 mW. Considering the pulsewidth $\tau_0 = 805$ ps, the highest peak power about 112 W is achieved at $P_p = 247$ mW.

4. Conclusions

The lasing characteristic of a low repetition rate mode-locked Yb-doped fiber laser with an all-normal dispersion cavity and mode-locked by the nonlinear polarization rotation (NPR) mechanism has been investigated in the present work. Although a numerical result [18] has shown that a stable single mode-locked pulse can hardly be achieved in an NPE laser with a cavity length of greater than 100 m, we add

a section of 520 m long single mode fiber inside the laser cavity to produce a 365 kHz low pulse repetition rate and also choose a 90/10 coupler for output coupling to produce a stable single mode-locked pulse. Without focusing the relatively high mode-locked pulse energy of the 4 μJ was generated using an 8 km ultra-long cavity YDFL in [15]. In this work, we study the evolution of a low repetition rate mode-locked laser transfer from the CM state to the ML state and find two different evolution routes as the pump power increases. In the first route, the laser transits to the Q-switched mode-locking state before complete mode-locked pulse generation. In the mode-locked state, the highest output power is about 34.5 mW, corresponding to 97.3 nJ highest pulse energy obtained at 228 mW pump power. In the other evolution route, the laser directly transfers from the CW state to the ML state with a sudden power jump as the pump power increases, and transfers back to the CW state with a sudden power drop as the pump power declines. A clear hysteresis phenomenon is observed for the first time, which must be closely related to the nonlinear gain/loss dynamics in the current laser system. Without dispersion compensation elements inside the laser cavity, the mode-locked pulses have sub-nanosecond pulsewidth. The linear dependence of pulsewidth on bandwidth under different pump powers indicates the presence of giant linear chirps from such a long cavity-length laser.

Acknowledgments

This work is financially sponsored by the National Science Council in Taiwan, ROC, under grant nos NSC 99-2112-M-027-001-MY3 and NSC 99-2221-E-009-045 MY3.

References

[1] Kobtsev S M, Kukarin S V and Fedotov Y S 2010 *Laser Phys.* **20** 347
[2] Tamura K, Ippen E P, Haus H A and Nelson L E 1993 *Opt. Lett.* **18** 1080
[3] Ilday F O, Buckley J R, Clark W G and Wise F W 2004 *Phys. Rev. Lett.* **92** 213902
[4] Lin K H, Lin J H and Chen C C 2010 *Laser Phys.* **20** 1984
[5] Kieu K and Wise F W 2008 *Opt. Express* **16** 11453
[6] Zhao L M, Tang D Y, Zhang H, Wu X, Bao Q and Loh K P 2010 *Opt. Lett.* **35** 3622
[7] Aguergaray C, Broderick N G R, Erkintalo M, Chen J S Y and Kruglov V 2012 *Opt. Express* **20** 10545
[8] Chong A, Buckley J, Renninger W and Wise F 2006 *Opt. Express* **14** 10095
[9] Chong A, Renninger W H and Wise F W 2007 *Opt. Lett.* **32** 2408
[10] Zhou H, Li W X and Zeng H P 2011 *Laser Phys.* **21** 399
[11] Zhang M, Chen L L, Zhou C, Cai Y, Ren L and Zhang Z G 2009 *Laser Phys. Lett.* **6** 657
[12] Tian X, Tang M, Cheng X, Shum P, Gong Y and Lin C 2009 *Opt. Express* **17** 7222
[13] Kong L J, Xiao X S and Yang C X 2010 *Laser Phys. Lett.* **7** 359
[14] Lin J H, Wang D and Lin K H 2011 *Laser Phys. Lett.* **8** 66
[15] Kobtsev S M, Kukarin S V, Smirnov S V and Fedotov Y S 2010 *Laser Phys.* **20** 351
[16] Wu X, Tang D Y, Zhang H and Zhao L M 2009 *Opt. Express* **17** 5580
[17] Liu X, Wang L, Li X, Sun H, Lin A, Lu K, Wang Y and Zhao W 2009 *Opt. Express* **17** 8506
[18] Kobtsev S M and Smirnov S V 2011 *Laser Phys.* **21** 272
[19] Lin J H, Lin K H, Hsu C C, Yang W H and Hsieh W F 2007 *Laser Phys. Lett.* **4** 413
[20] Zhang G, Zhao S Z, Li Y F, Li G Q, Li D C and Yang K J 2009 *Laser Phys.* **19** 2082
[21] Yen T H, Lin J H and Lai Y 2012 *Laser Phys.* **22** 441
[22] Honninger C, Paschotta R, Morier-Genoud F, Moser M and Keller U 1999 *J. Opt. Soc. Am.* B **16** 466